Author Manuscript

Author Manuscript

Author Manuscript

Author Manuscript

HHS Public Access

Author manuscript

Gastro Hep Adv. Author manuscript; available in PMC 2023 January 11.

Published in final edited form as:

Gastro Hep Adv. 2023 ; 2(1): 96–107. doi:10.1016/j.gastha.2022.09.004.

A20 Restricts NOS2 Expression and Intestinal Tumorigenesis in a Mouse Model of Colitis-Associated Cancer

David W. Basta,

Mandy Vong,

Adolat Beshimova,

Brooke N. Nakamura,

Iulia Rusu,

Michael G. Kattah,

Ling Shao

Division of Gastroenterology and Liver Disease, Department of Medicine, University of Southern California, Keck School of Medicine, Los Angeles, California

Abstract

BACKGROUND AND AIMS: Colon cancer can occur sporadically or in the setting of chronic inflammation, such as in patients with inflammatory bowel disease. We previously showed that A20, a critical negative regulator of tumor necrosis factor signal transduction, could regulate sporadic colon cancer development. In this report, we investigate whether A20 also acts as a tumor suppressor in a model of colitis-associated cancer.

METHODS: Colitis and colitis-associated tumors were induced in wild-type and A20 intestinal epithelial cell-specific knockout (A20dIEC) mice using dextran sodium sulfate and azoxymethane. Clinicopathologic markers of inflammation were assessed in conjunction with colonic tumor burden. Gene expression analyses and immunohistochemistry were performed on colonic tissue and intestinal enteroids. Nitric oxide (NO) production and activity were assessed in whole colonic lysates and mouse embryonic fibroblasts.

This is an open access article under the CC BY-NC-ND license (http://creativecommons.org/licenses/by-nc-nd/4.0/).

Correspondence: Address correspondence to: Ling Shao, MD, PhD, Division of Gastroenterology and Liver Disease, Department of Medicine, University of Southern California, Keck School of Medicine, 2011 Zonal Avenue, Hoffman Medical Research 600, Los Angeles, California 90033. lingshao76@gmail.com.

Authors' Contributions:

David W. Basta, Brooke N. Nakamura, and Ling Shao conceived and designed the study. David W. Basta, Mandy Vong, Adolat Beshimova, Brooke N. Nakamura, Iulia Rusu, Michael G. Kattah, and Ling Shao participated in the generation, collection, assembly, analysis, and interpretation of data. David W. Basta, Brooke N. Nakamura, and Ling Shao wrote the manuscript. All authors had access to the study data, had reviewed the final manuscript, and approved the final version of the manuscript.

Conflicts of Interest:

The authors disclose no conflicts.

Ethical Statement:

The corresponding author, on behalf of all authors, jointly and severally, certifies that their institution has approved the protocol for any investigation involving humans or animals and that all experimentation was conducted in conformity with ethical and humane principles of research.

Data Transparency Statement:

Study material will be made available upon request from the corresponding author.

Author Manuscript Author Manuscript Author Manuscript Author Manuscript

RESULTS: A20dIEC mice develop larger tumors after treatment with dextran sodium sulfate and azoxymethane than wild-type mice. In addition to elevated markers of inflammation, A20dIEC mice have significantly enhanced expression of inducible nitric oxide synthase (iNOS), a well-known driver of neoplasia. Enhanced iNOS expression is associated with the formation of reactive nitrogen species and DNA damage. Loss of A20 also enhances NO-dependent cell death directly.

CONCLUSION: Mechanistically, we propose that A20 normally restricts tumor necrosis factor–induced nuclear factor kappa B–dependent production of iNOS in intestinal epithelial cells, thereby protecting against colitis-associated tumorigenesis. We also propose that A20 plays a direct role in regulating NO-dependent cell death.

Keywords

Colon; Ulcerative colitis; Inflammation; Nitric oxide; A20; Tnfaip3; Tumor

Introduction

Colorectal cancer (CRC) is the third most common cancer and the third leading cause of cancer-related death in the United States. CRC accounts for over 50000 deaths in the United States annually, while in 2017, the National Cancer Institute estimated that there were over 1 million Americans living with CRC. Although mortality from CRC has been declining overall in the United States, death rates are rising among younger individuals.[1] CRC is also more common among African Americans and significant disparities in outcomes exist based on race and ethnicity, as well as socioeconomic status.[2] Recent estimates suggest that the economic burden of CRC exceeded $16 billion in 2018.[3] Overall, CRC remains a significant problem and new treatments are still needed.

CRC can occur sporadically in the general population or can be associated with chronic inflammation. One well-known predisposing factor associated with CRC development is inflammatory bowel disease (IBD). Patients with IBD have as much as a six-fold increased risk of developing CRC compared to the general population.[4,5] Moreover, this colitis-associated cancer accounts for 10%–15% of the mortality associated with IBD.[6]

The pathophysiology of sporadic colon cancers and colitis-associated cancers is distinct. Seminal work from Dr Vogelstein and colleagues demonstrated a sequence of mutations commonly found in sporadic colon cancers proceeding from an initiating mutation in adenomatous polyposis coli (APC) progressing to mutations in Kirsten rat sarcoma virus and finally, p53.[7-11] Studies in colitis-associated cancer show that specific genetic mutations also correlate with the adenoma to carcinoma progression[12]; however, the nature and order of these mutations are altered. Indeed, in contrast to sporadic colon cancers, loss of p53 appears to be an early event in colitis-associated cancers and is seen in up to a third of biopsy specimens with only low-grade dysplasia.[13,14] In contrast, APC mutations are uncommon in colitis-associated cancers and dysplasia, occurring in less than 10% of cases in some series.[15,16]

Colitis-associated cancers may be accelerated by dysregulation of the nuclear factor kappa B (NFkB) signaling pathway. The NFkB pathway is a critical regulator of both

Author Manuscript Author Manuscript Author Manuscript Author Manuscript

inflammation and cell death.[17,18] Major activators of NFkB are the tumor necrosis factor (TNF) superfamily, including TNF, TRAIL, and FAS, as well as the Toll-like receptor family and reactive oxygen species.[19] Multiple studies have shown that tumor growth and neoplastic progression depend on NFkB signals.[20] NFkB p65 has been shown to be overexpressed in human CRC tissues,[21] potentially enhancing tumorigenesis by upregulating antiapoptotic genes. Additionally, overactivity of the NFkB pathway is sufficient to drive colon carcinogenesis in mice.[22]

A20, encoded by TNF alpha-induced protein 3 (TNFAIP3), is a ubiquitin binding and editing enzyme that negatively regulates inflammation.[23-25] Defects in A20 in humans cause a systemic inflammatory syndrome, while A20 defects in mice cause early lethality due to widespread inflammation.[26,27] A20 has been shown to be a critical regulator of NFkB signaling through the regulation of proximal TNF-receptor signaling.[23,28] Of note, although the majority of the literature supports the role of A20 as a negative regulator of inflammation and apoptosis, a recent report demonstrated that, conversely, overexpression of A20 can promote TNF-induced and receptor interacting serine/threonine kinase 1-dependent inflammation and apoptosis in intestinal epithelial cells (IECs).[29]

A20 is a tumor suppressor for multiple types of malignancy. Deletion or downregulation of A20 has been found in multiple B-cell lymphoma subtypes.[30-34] Similarly, A20 dysregulation has been shown to contribute to the initiation or progression of gastric cancer,[35,36] breast cancer,[37] esophageal cancer,[38,39] thyroid cancer,[40] and colon cancer.[41,42] We previously reported that A20 could act as a tumor suppressor in a murine model of sporadic CRC.[42]

In this report, we investigated the effect of IEC-specific A20 deletion in a well-characterized dextran sodium sulfate and azoxymethane (AOM-DSS) model of colitis-associated cancer. We found that epithelial A20 knockout mice had increased tumor burden. Enteroid cultures from A20 knockout mice revealed strong induction of inducible nitric oxide synthase (iNOS) in response to inflammatory signals, which were confirmed in vivo. In addition to restricting TNF-induced iNOS, we also show that A20 may directly regulate nitric oxide (NO)-dependent cell death.

Results

To investigate the role of A20 in colitis-associated cancer, we used a mouse strain with an intestinal epithelial cell-specific knockout of A20 (A20dIEC). Eight- to twelve-week-old wild-type (WT) and A20dIEC mice were treated with the mutagen AOM-DSS to induce colitis-associated tumorigenesis. AOM was administered on day 0 followed by 3 rounds of DSS treatment, each lasting 5 days and separated by a 16-day rest period (Figure 1A). Mice were culled after the final rest period on day 70, and the colon, spleen, mesenteric lymph nodes, and serum were harvested for downstream analyses.

We observed no significant differences between WT and A20dIEC mice when assessing traditional markers of DSS-induced intestinal inflammation, including weight loss, colon length, spleen weight, or clinical score (Figure 1B-E). However, A20dIEC mice appeared

Author Manuscript Author Manuscript Author Manuscript Author Manuscript

to have a generally more immunoreactive profile compared to WT mice after AOM-DSS treatment, as suggested by significantly higher serum levels of TNF and elevated IL-12 (Figure 1F and G). Additionally, A20dIEC mice had lower levels of naive splenic CD4 T cells and higher levels of activated splenic monocytes (Figure 1H and I). Together, these results suggest that loss of A20 expression specifically in IECs supports systemic immune activation in the AOM-DSS colitis model of colon cancer, although loss of A20 does not result in worsening of traditional clinicopathologic markers of DSS-induced intestinal inflammation under our experimental conditions.

WT and A20dIEC mice had similar numbers of colonic tumors on day 70 (Figure 2A). However, despite similar tumor numbers, the average tumor size was larger in A20dIEC mice compared to WT, resulting in an increased tumor burden (Figure 2B and C). Histologic examination revealed that colonic tumors were grossly similar between WT and A20dIEC mice in regard to the severity of dysplasia and the level of invasiveness (Figure 2D-I). These results suggest that A20 slows tumor growth and overall tumor burden without affecting tumor formation in the AOM-DSS colitis model of colon cancer.

To identify molecular mechanisms underlying the increased tumor burden in A20dIEC mice, we first measured global gene expression using RNA-seq in WT and A20dIEC-derived small intestinal enteroids stimulated with TNF. Among the most differentially expressed genes was *NOS2*, encoding the iNOS. Reads mapping to *NOS2* were significantly enriched in A20dIEC mice compared to WT (Figure 3A). We also confirmed increased expression of NOS2 in A20dIEC-derived colonic enteroids by qRT-PCR under both TNF-stimulated and unstimulated conditions (Figure 3B). Importantly, expression of TNFAIP3, the gene encoding A20, was detected only in WT colonic enteroids, where its expression increased in a TNF-dependent manner (Figure 3C). This finding confirmed that A20 was successfully depleted in our A20dIEC-derived colonic enteroids and that its expression is controlled by TNF signaling under our experimental conditions. We also observed increased expression of IkBa in A20dIEC-derived colonic enteroids (Figure 3D). IkBa is positively regulated by NFkB and served as a positive control for TNF stimulation.[43] Increased NOS2 gene expression was correlated with increased iNOS functional activity, as measured by a TNF-dependent increase in the reactive nitrogen species (RNS) nitrite, specifically in the supernatant of A20dIEC-derived colonic enteroids (Figure 3E). To determine whether the increased NOS2 expression in A20dIEC-derived colonic enteroids is associated with elevated expression of iNOS in vivo, we measured iNOS protein levels by Western blot in IEC extracts isolated from colonic tissue of WT and A20dIEC mice treated with one round of DSS. We observed a DSS-dependent increase in expression of iNOS in A20dIEC mice relative to WT (Figure 4A). Increased expression was corroborated by immunohistochemical staining of tissue sections of colonic epithelium (Figure 4B and C). Surprisingly, iNOS expression in A20dIEC mice was significantly increased compared to WT in the normal colonic epithelium but not in sections of colonic tumors (data not shown). Based on these results, we conclude that A20 negatively regulates NOS2 gene expression and RNS production in intestinal tissues, potentially via inhibition of NFkB signaling.

RNS are known to cause DNA damage and apoptosis, contributing to tumor formation and tumor progression.[44] Accordingly, we observed increased expression of the DNA damage

Author Manuscript Author Manuscript Author Manuscript Author Manuscript

marker p53 in whole colonic lysates from A20dIEC mice (Figure 5A). We also found that A20-deficient mouse embryonic fibroblasts showed increased cell death when treated with exogenous NO (Figure 5B). This latter finding was surprising because it suggests that in addition to regulating the production of RNS via NOS2 gene expression, A20 independently protects cells against RNS-mediated toxicity. In agreement with this finding, loss of A20 was associated with enhanced activation of intrinsic apoptosis in the presence of NO in both mouse embryonic fibroblasts and colonic enteroids (Figure 5C-F). Together, these findings suggest that A20 protects against RNS-mediated DNA damage and apoptosis in the setting of colitis-associated cancer and provide a potential explanation for the increased tumor burden in mice lacking this critical regulator.

Discussion

The underlying pathophysiology of colon cancers that arise in the setting of inflammation is poorly understood. One factor that may play a role is abnormal production or function of the small molecule NO. NO is produced by 3 isozymes of nitric oxide synthase, nNOS/NOS1, iNOS/NOS2, and eNOS/NOS3. Previous reports have shown focal NO induction in the intestinal epithelium of patients with ulcerative colitis,[45] and our data strongly corroborate the role of enhanced NO production in the setting of chronic inflammation. The fact that our final tissue analysis was performed 16 days after the final DSS cycle (Figure 4B and C) also suggests that a sustained upregulation of iNOS occurs in A20dIEC mice. Taken together, our data support the usefulness of the AOM-DSS model for studying A20-regulated NO production and activity in the intestine.

NO may promote CRC development through multiple mechanisms. RNS such as peroxynitrite can cause DNA mutations directly but may also inhibit the function of DNA repair proteins or stimulate angiogenesis.[46-48] Additionally, NO may induce cell death directly through a mitochondrial-dependent pathway.[49] Our data show that loss of A20 may facilitate carcinogenesis by potentiating the expression of iNOS and by enhancing the lethality of the resulting increase in NO production.

Excess apoptosis has been noted in inflammatory diseases such as IBD[50,51] and graft-versus-host disease,[52,53] while dysregulated apoptosis could contribute to the development of CRC.[54] Our finding that A20 may regulate NO-induced apoptosis independently of its role in regulating NO production is intriguing as a potential contributor to these conditions. Although low levels of NO are known to inhibit apoptosis, high levels can trigger apoptosis through multiple mechanisms.[55] Covalent incorporation of NO (s-nitrosylation) has been shown to alter the function of death receptors such as TRAIL[56] and FAS[57] but can also alter the function of downstream death-inducing molecules including the proapoptotic caspase-3 and caspase-8.[58] Alternatively, s-nitrosylation of NFkB can inhibit the expression of antiapoptotic proteins.[59] A20 could potentially regulate NO-induced cell death through dysregulation of NFkB signaling or alternatively through its known roles in regulating caspase-8 containing death complexes via regulation of receptor interacting serine/threonine kinase 1.[23,25,60,61] However, a detailed mechanistic explanation of the regulatory role A20 plays in apoptosis is the subject of ongoing investigations.

Author Manuscript Author Manuscript Author Manuscript Author Manuscript

Surprisingly, iNOS expression was specifically increased in the normal surrounding colonic epithelium but not within the tumors of A20dIEC mice relative to WT (Figure 4B and C and data not shown). This finding suggests that increased iNOS expression may promote early tumor formation in normal colonic epithelium but may play a less important role in tumor progression. However, our finding that the total number of tumors was similar between WT and A20dIEC mice at the end of the experiment seemingly contradicts this notion (Figure 2A). The observed increase in tumor size despite similar tumor numbers instead suggests that increased iNOS expression accelerates tumor progression without affecting net tumor incidence. A careful examination of the dynamics of tumor formation and progression will shed more light on this observation and perhaps resolve the apparent discrepancy.

Overall, our findings suggest that A20 acts as a tumor suppressor in colitis-associated cancers by regulating NFkB-dependent expression of iNOS and the ensuing production of RNS. Although direct inhibition of NO production would likely have pleiotropic effects, our results raise the intriguing possibility that inhibition of iNOS activity, or the quenching of RNS byproducts, could serve an adjunctive therapeutic role in the treatment of colitis-associated cancer. Additionally, our findings support an independent role for A20 in protecting cells against RNS-mediated lethality (Figure 6).

Methods

Antibodies and Reagents

DETA-NONOate was obtained from Abcam (Cambridge, United Kingdom). Antibodies to A20, cleaved-caspase 3, iNOS, and PARP were obtained from Cell Signaling Technologies (Danvers, MA). GAPDH was obtained from Millipore Sigma (Burlington, MA). p53 was obtained from Santa Cruz Biotechnology (Dallas, TX). Anti-rabbit Cy3 was obtained from Jackson ImmunoResearch (West Grove, PA). DAPI and Phalloidin were obtained from Thermo Fisher Scientific and Abcam, respectively. Recombinant mTNF was obtained from R&D Systems (Minneapolis, MN). Cycloheximide was obtained from Sigma-Aldrich (St. Louis, MO). Cell Titer Glo was obtained from Promega (Madison, WI). DSS 40 kDa was obtained from Chem-Impex Int'l INC (Wood Dale, IL). AOM was obtained from Sigma (St. Louis, MO).

Mice: $A20^{FL}$ mice were generated as described previously.[62] WT and A20-deficient mouse embryonic fibroblasts were generated as described previously.[63] Villin-Cre mice were purchased from Jackson Labs. Villin-ERT2-Cre mice were originally obtained from Dr Sylvie Robine.[64]

Induction of Colitis-Associated Tumors

AOM was injected intraperitoneally into eight- to twelve-week-old WT and A20dIEC mice at a concentration of 10 mg/kg body weight on experimental day 0. 3 cycles of DSS were administered at a concentration of 1.75%. Tumor number and burden were determined at 4 months of age with the aid of a stereomicroscope equipped with a sizing reticle (Klarman Rulings, Litchfield, NH). The clinical score was calculated as the average of the combined score of weight loss, stool consistency, and bleeding following each DSS cycle. Each

Author Manuscript Author Manuscript Author Manuscript Author Manuscript

category was scored as followed: weight loss: 0 (no loss), 1 (1%–5%), 2 (5%–10%), 3 (10%–20%), and 4 (>20%); stool consistency: 0 (normal), 2 (loose stool), and 4 (diarrhea); and bleeding: 0 (no blood), 2 (visual blood on bedding), and 4 (gross bleeding, blood around anus).[65] All animal studies were conducted in accordance with the University of Southern California (IACUC #20192) Institutional Animal Care and Use Committee.

Histology/Immunohistochemistry

Formalin-fixed paraffin sections were deparaffinized and rehydrated. Antigen retrieval was performed with 10 mM sodium citrate buffer, pH 6.0 in a 95 °C water bath for 30 minutes. Tissue was permeabilized with 0.3% Tween-20 in 1× phosphate-buffered saline (PBS) for 45 minutes at 37 °C. Sections were blocked using SEA BLOCK Blocking Buffer (Thermo Fisher, Waltham, MA) for 1 hour at room temperature. Primary antibodies were incubated overnight at 4 °C in blocking buffer. Slides were incubated for 1 hour at room temperature with secondary antibody and counter stained with Phalloidin-iFluor 488 (Abcam) and DAPI (Thermo Fisher) and mounted with ProLong Gold (ThermoFisher) and glass coverslips sealed with nail polish. Images were captured using a Leica TCS SP5 multiphoton confocal microscope and quantified using Fiji.[66] iNOS fluorescence was quantified by normalizing the total integrated density (Alexa 594) to the total surface area of colonic epithelium.

Flow Cytometry

Cells were resuspended to a concentration of 1×10^6 cells/ml. Cells were stained with antibodies CD44-FITC, CD69-PE, CD4-PE/Cy7, CD62L-APC, CD8-vFluor450, CD25-APC/Cy7, CD80-FITC, CD86-PE, CD11b-PE/Cy7, F4/80-APC, IA/E-vFluor 450, GR 1-APC/Cy7, and B220-PerCP/Cy5.5 (Tonbo Bioscience, San Diego, CA) and Zombie Yellow Fixable Viability Kit (BioLegend). Cells were incubated in the dark at room temperature for 30 minutes. Flow cytometry acquisition was performed on a FacsVantage (BD Biosciences, San Jose, CA) and analyzed using FlowJo software (BD Biosciences, San Jose, CA).

Enzyme-Linked Immunosorbent Assay

IL-12 and TNF cytokine enzyme-linked immunosorbent assay was performed according to the manufacturer's instructions (PeproTech, Cranbury, NJ). Briefly, enzyme-linked immunosorbent assay plates (Corning) were coated with capture antibody diluted to 1 μg/ml. Nonspecific binding was blocked using PBS containing 1% bovine serum albumin (Sigma). Cell supernatants were added and incubated at room temperature for 2 hours. Detection antibody was added at a concentration of 500 ng/ml for 2 hours, followed by an avidin-horseradish peroxidase conjugate at a dilution of 1:2000 for 30 minutes. Plates were washed between each step 5× with PBS containing 0.05% Tween-20 (Sigma P9416). Plates were developed using TMB substrate and read using a Fluostar Omega (BMG Labtech, Cary, NC).

Enteroids

Large and small intestine enteroids were isolated as previously described.[67,68] A20FL/FL VillinERCre$^+$ and A20FL/FL VillinERCre$^-$ mice were euthanized according to IACUC-approved protocols. Colons and small intestines from each mouse were removed and gently

Author Manuscript Author Manuscript Author Manuscript Author Manuscript

flushed with cold PBS. They were then cut open lengthwise and cut into 2 mm pieces. Intestinal pieces were washed 15× with ice-cold PBS by pipetting the suspended pieces up and down 3 times. Tissue pieces were then incubated in Gentle Cell Dissociation Reagent (StemCell) for 20 minutes at room temperature. Fractions were then collected from the intestinal pieces in 0.1% bovine serum albumin/PBS. Fractions that contained crypts were used for enteroid culture. The crypts were resuspended in a 1:1 mixture of Matrigel (Corning) and complete IntestiCult Media (StemCell), which was then plated in a prewarmed 24-well plate and covered with 750 μl complete IntestiCult. The medium was changed every 2–3 days and enteroids were split every 7–10 days. Enteroids were incubated with 4-OH tamoxifen for 72 hours to knockout A20. Following knockout, enteroids were treated with recombinant murine TNF at 10 ng/ml in complete IntestiCult for 24 hours.

Nitrite Measurement

Total nitrite concentrations were measured via Parameter kit (R&D systems) according to the manufacturer's instructions. Briefly, dilutions of supernatants from enteroid cultures, standards, or blanks were added to 96-well plates. Griess reagents I and II were added and incubated for 10 minutes at room temperature. Optical density of each sample was recorded at both 540 and 690 nm on a Fluostar Omega plate reader.

Western Blot

Colonic tissue was flash frozen in liquid nitrogen and homogenized using a mortar and pestle. For Western blot, pellets from these homogenates were lysed in ice-cold buffer containing 200 μg/ml digitonin (150 mM NaCl and 50 mM HEPES) and the Roche complete mini protease inhibitor cocktail for 20 minutes, then cleared by centrifugation. Lysates were prepared identically for enteroids and mouse embryonic fibroblasts. Protein concentrations were determined by bicinchoninic acid assay (Thermo). Samples were mixed with NuPage loading buffer and NuPage sample reducing agent (Invitrogen) and resolved on 4%–12% Bis-Tris (Invitrogen) gels, then transferred to 0.4 μM polyvinylidene fluoride (Millipore). Western blot development was performed using the Clarity chemiluminescent substrate (Bio-Rad, Hercules, CA) and imaged on a ChemiDoc Touch (Bio-Rad) system. Analysis was performed using Image Lab (Bio-Rad).

RNA-Seq

Total RNA was isolated using the RNeasy Plus Mini Kit (Qiagen, Hilden, Germany). RNA quality was determined by Bioanalyzer 2100 (Agilent, Santa Clara, CA). Libraries were prepared from 500 ng of total RNA using a Kapa mRNA HyperPrep Kit for Illumina platforms (Kapa Biosystems, Inc., Wilmington, MA). Final library products were quantified using the Qubit 2.0 Fluorometer (Thermo Fisher Scientific Inc., Waltham, MA), and the fragment size distribution was determined with the Bioanalyzer 2100. Equimolar concentrations of the libraries were then pooled and the final pool was quantified via qPCR using the Kapa Biosystems Library Quantification Kit according to the manufacturer's instructions. The pool was sequenced in an Illumina HiSeq 2500 platform (Illumina, San Diego, CA) in Rapid Single-Read 75 cycles format, targeting at least 30 million reads per sample. The preparation of the libraries and the sequencing was performed at the UPC Genome Core (University of Southern California, Los Angeles, CA).

Author Manuscript Author Manuscript Author Manuscript Author Manuscript

Initial read quality and adaptor content of FASTQ files were assessed with FastQC.[69] Reads were then trimmed based on quality score and adaptor sequences removed using Trimmomatic.[70] After filtering, surviving reads were checked again in FastQC to ensure that only high-quality transcriptome reads were put into the analysis pipeline. These high-quality reads were mapped to the human genome (ver. GRCh38.p7) using the ultra-fast aligner STAR[71]; the same software was used to obtain uniquely mapping read counts for each gene feature included in a gene transfer format (GTF) file. Both the genome and the GTF file were downloaded from the GENCODE database (https://www.gencodegenes.org).

Quantitative PCR

mRNA was extracted using Trizol (Invitrogen) and the DirectZol column purification kit (Zymo). First strand cDNA synthesis was performed using Maxima H- Mastermix (Thermo). Primers to NOS2, A20, and NFKBIA were designed using IDT Primer Quest (Table 1). Quantitative PCR was performed using TB Green Premix Ex Taq II Rox plus (Takara, Japan, Lot #AJF1254A) and run on a CFX-384 Touch Real-Time PCR Detection System (Bio-Rad).

Statistical Analysis

Statistical analysis was performed with GraphPad Prism 4 (GraphPad Software, San Diego, CA). Comparisons between 2 groups were performed by two-tailed unpaired Student's *t*-test. Multigroup comparisons were performed by one-way analysis of variance. $P < .05$ was used as the threshold for statistical significance. All experiments shown are representative of at least 3 independent experiments.

All authors had access to the study data and had reviewed and approved the final manuscript.

Funding:

This work was supported by NIH R03 DK118178 (L.S.). Additional support was provided by the USC Research Center for Liver Disease P30 DK048522 and the Norris Cancer Center P30 CA014089.

Abbreviations used in this paper:

A20dIEC	A20 intestinal epithelial cell-specific knockout
AOM-DSS	dextran sodium sulfate and azoxymethane
APC	adenomatous polyposis coli
CRC	colorectal cancer
GTF	gene transfer format
IBD	inflammatory bowel disease
iNOS	nitric oxide synthase
NO	nitric oxide
NFkB	nuclear factor kappa B

Author Manuscript Author Manuscript Author Manuscript Author Manuscript

PBS	phosphate-buffered saline
RNS	reactive nitrogen species
TNF	tumor necrosis factor
WT	wild type

References

1. Siegel RL, Miller KD, Goding Sauer A, et al. Colorectal cancer statistics, 2020. CA Cancer J Clin 2020;70:145–164. [PubMed: 32133645]
2. Zavala VA, Bracci PM, Carethers JM, et al. Cancer health disparities in racial/ethnic minorities in the United States. Br J Cancer 2021;124:315–332. [PubMed: 32901135]
3. "Cancer trends progress report". Bethesda, Maryland: National Cancer Institute, NIH, DHHS, 2020.
4. Bae SI, Kim YS. Colon cancer Screening and Surveillance in inflammatory bowel disease. Clin Endosc 2014;47:509. [PubMed: 25505716]
5. Beaugerie L, Svrcek M, Seksik P, et al. Risk of colorectal high-grade dysplasia and cancer in a prospective observational Cohort of patients with inflammatory bowel disease. Gastroenterology 2013;145:166–175.e8. [PubMed: 23541909]
6. Mattar MC, Lough D, Pishvaian MJ, Charabaty A. Current management of inflammatory bowel disease and colorectal cancer. Gastrointest Cancer Res GCR 2011;4:53–61. [PubMed: 21673876]
7. Vogelstein B, Fearon ER, Hamilton SR, et al. Genetic alterations during colorectal-tumor development. N Engl J Med 1988;319:525–532. [PubMed: 2841597]
8. Baker S, Fearon E, Nigro J, et al. Chromosome 17 deletions and p53 gene mutations in colorectal carcinomas. Science 1989;244:217–221. [PubMed: 2649981]
9. Fearon E, Cho K, Nigro J, et al. Identification of a chromosome 18q gene that is altered in colorectal cancers. Science 1990;247:49–56. [PubMed: 2294591]
10. Powell SM, Zilz N, Beazer-Barclay Y, et al. APC mutations occur early during colorectal tumorigenesis. Nature 1992;359:235–237. [PubMed: 1528264]
11. Fearon ER, Vogelstein B. A genetic model for colorectal tumorigenesis. Cell 1990;61:759–767. [PubMed: 2188735]
12. Redston MS, Papadopoulos N, Caldas C, et al. Common occurrence of APC and K-ras gene mutations in the spectrum of colitis-associated neoplasias. Gastroenterology 1995;108:383–392. [PubMed: 7835579]
13. Gibson PR, Folino M, Rosella O, et al. Neoplasia and hyperplasia of large bowel: focal lesions in an abnormal epithelium. Gastroenterology 1992;103:1452–1459. [PubMed: 1358742]
14. Brentnall TA, Crispin DA, Rabinovitch PS, et al. Mutations in the p53 gene: an early marker of neoplastic progression in ulcerative colitis. Gastroenterology 1994;107:369–378. [PubMed: 8039614]
15. Tarmin L, Yin J, Harpaz N, et al. Adenomatous polyposis coli gene mutations in ulcerative colitis-associated dysplasias and cancers versus sporadic colon neoplasms. Cancer Res 1995;55:2035–2038. [PubMed: 7743497]
16. Fogt F, Vortmeyer AO, Goldman H, et al. Comparison of genetic alterations in colonic adenoma and ulcerative colitis-associated dysplasia and carcinoma. Hum Pathol 1998;29:131–136. [PubMed: 9490271]
17. Taniguchi K, Karin M. NF-κB, inflammation, immunity and cancer: coming of age. Nat Rev Immunol 2018;18:309–324. [PubMed: 29379212]
18. Luo J-L, Kamata H, Karin M. IKK/NF-kappaB signaling: balancing life and death–a new approach to cancer therapy. J Clin Invest 2005;115:2625–2632. [PubMed: 16200195]
19. Temkin V, Karin M. From death receptor to reactive oxygen species and c-Jun N-terminal protein kinase: the receptor-interacting protein 1 odyssey. Immunol Rev 2007;220:8–21. [PubMed: 17979836]

Author Manuscript Author Manuscript Author Manuscript Author Manuscript

20. Xu H, Liu L, Li W, et al. Transcription factors in colorectal cancer: molecular mechanism and therapeutic implications. Oncogene 2021;40:1555–1569. [PubMed: 33323976]
21. Yu L-L, Yu HG, Yu JP, et al. Nuclear factor-kappaB p65 (RelA) transcription factor is constitutively activated in human colorectal carcinoma tissue. World J Gastroenterol 2004;10:3255–3260. [PubMed: 15484295]
22. Greten FR, Eckmann L, Greten TF, et al. IKKbeta links inflammation and tumorigenesis in a mouse model of colitis-associated cancer. Cell 2004;118:285–296. [PubMed: 15294155]
23. Shembade N, Ma A, Harhaj EW. Inhibition of NF- B signaling by A20 through Disruption of ubiquitin enzyme complexes. Science 2010;327:1135–1139. [PubMed: 20185725]
24. Boone DL, Turer EE, Lee EG, et al. The ubiquitin-modifying enzyme A20 is required for termination of Toll-like receptor responses. Nat Immunol 2004;5:1052–1060. [PubMed: 15334086]
25. Wertz IE, O'Rourke KM, Zhou H, et al. De-ubiquitination and ubiquitin ligase domains of A20 downregulate NF-κB signalling. Nature 2004;430:694–699. [PubMed: 15258597]
26. Zhou Q, Wang H, Schwartz DM, et al. Loss-of-function mutations in TNFAIP3 leading to A20 haploinsufficiency cause an early-onset autoinflammatory disease. Nat Genet 2016;48:67–73. [PubMed: 26642243]
27. Lee EG, Boone DL, Chai S, et al. Failure to regulate TNF-induced NF-kappaB and cell death responses in A20-deficient mice. Science 2000;289:2350–2354. [PubMed: 11009421]
28. Tokunaga F, Nishimasu H, Ishitani R, et al. Specific recognition of linear polyubiquitin by A20 zinc finger 7 is involved in NF-κB regulation. EMBO J 2012;31:3856–3870. [PubMed: 23032187]
29. Garcia-Carbonell R, Wong J, Kim JY, et al. Elevated A20 promotes TNF-induced and RIPK1-dependent intestinal epithelial cell death. Proc Natl Acad Sci 2018;115:E9192–E9200. [PubMed: 30209212]
30. Fan Z, Pei R, Sha K, et al. Comprehensive characterization of driver genes in diffuse large B cell lymphoma. Oncol Lett 2020;20:382–390.
31. Troppan K, Hofer S, Wenzl K, et al. Frequent down regulation of the tumor suppressor gene A20 in multiple Myeloma. PLoS One 2015;10:e0123922. [PubMed: 25856582]
32. Etzel B-M, Gerth M, Chen Y, et al. Mutation analysis of tumor necrosis factor alpha-induced protein 3 gene in Hodgkin lymphoma. Pathol Res Pract 2017;213:256–260. [PubMed: 28189285]
33. Kato M, Sanada M, Kato I, et al. Frequent inactivation of A20 in B-cell lymphomas. Nature 2009;459:712–716. [PubMed: 19412163]
34. Schmitz R, Hansmann ML, Bohle V, et al. TNFAIP3 (A20) is a tumor suppressor gene in Hodgkin lymphoma and primary mediastinal B cell lymphoma. J Exp Med 2009;206:981–989. [PubMed: 19380639]
35. Du B, Liu M, Li C, et al. The potential role of TNFAIP3 in malignant transformation of gastric carcinoma. Pathol Res Pract 2019;215:152471. [PubMed: 31153693]
36. West AC, Tang K, Tye H, et al. Identification of a TLR2-regulated gene signature associated with tumor cell growth in gastric cancer. Oncogene 2017;36:5134–5144. [PubMed: 28481875]
37. Lee J-H, Jung SM, Yang KM, et al. A20 promotes metastasis of aggressive basal-like breast cancers through multi-monoubiquitylation of Snail1. Nat Cell Biol 2017;19:1260–1273. [PubMed: 28892081]
38. Hadisaputri YE, Miyazaki T, Yokobori T, et al. TNFAIP3 overexpression is an independent factor for poor survival in esophageal squamous cell carcinoma. Int J Oncol 2017;50:1002–1010. [PubMed: 28197630]
39. Ghadban T, Schmidt-Yang M, Uzunoglu FG, et al. Evaluation of the germline single nucleotide polymorphism rs583522 in the TNFAIP3 gene as a prognostic marker in esophageal cancer. Cancer Genet 2015;208:595–601. [PubMed: 26598072]
40. Pitt SC, Hernandez RA, Nehs MA, et al. Identification of Novel Oncogenic mutations in thyroid cancer. J Am Coll Surg 2016;222:1036–1043.e2. [PubMed: 27010584]
41. Ungerbäck J, Belenki D, Jawad ul-Hassan A, et al. Genetic variation and alterations of genes involved in NFκB/TNFAIP3- and NLRP3-inflammasome signaling affect susceptibility and outcome of colorectal cancer. Carcinogenesis 2012;33:2126–2134. [PubMed: 22843550]

Author Manuscript Author Manuscript Author Manuscript Author Manuscript

42. Shao L, Oshima S, Duong B, et al. A20 restricts Wnt signaling in intestinal epithelial cells and Suppresses colon carcinogenesis. PLoS One 2013;8:e62223. [PubMed: 23671587]
43. Auphan N, DiDonato JA, Rosette C, et al. Immunosuppression by glucocorticoids: inhibition of NF-kappa B activity through induction of I kappa B synthesis. Science 1995;270:286–290. [PubMed: 7569976]
44. Wiseman H, Halliwell B. Damage to DNA by reactive oxygen and nitrogen species: role in inflammatory disease and progression to cancer. Biochem J 1996;313(Pt 1):17–29. [PubMed: 8546679]
45. Singer II, Kawka DW, Scott S, et al. Expression of inducible nitric oxide synthase and nitrotyrosine in colonic epithelium in inflammatory bowel disease. Gastroenterology 1996;111:871–885. [PubMed: 8831582]
46. Shapiro R, Dubelman S, Feinberg AM, et al. Isolation and identification of cross-linked nucleosides from nitrous acid treated deoxyribonucleic acid. J Am Chem Soc 1977;99:302–303. [PubMed: 830687]
47. Radi R, Beckman JS, Bush KM, et al. Peroxynitrite-induced membrane lipid peroxidation: the cytotoxic potential of superoxide and nitric oxide. Arch Biochem Biophys 1991;288:481–487. [PubMed: 1654835]
48. Wink DA, Laval J. The Fpg protein, a DNA repair enzyme, is inhibited by the biomediator nitric oxide in vitro and in vivo. Carcinogenesis 1994;15:2125–2129. [PubMed: 7955043]
49. Poderoso JJ, Helfenberger K, Poderoso C. The effect of nitric oxide on mitochondrial respiration. Nitric Oxide Biol Chem 2019;88:61–72.
50. Arai N, Mitomi H, Ohtani Y, et al. Enhanced epithelial cell turnover associated with p53 accumulation and high p21WAF1/CIP1 expression in ulcerative colitis. Mod Pathol 1999;12:604–611. [PubMed: 10392637]
51. Iwamoto M, Koji T, Makiyama K, et al. Apoptosis of crypt epithelial cells in ulcerative colitis. J Pathol 1996;180:152–159. [PubMed: 8976873]
52. Ponec RJ, Hackman RC, McDonald GB. Endoscopic and histologic diagnosis of intestinal graft-versus-host disease after marrow transplantation. Gastrointest Endosc 1999;49:612–621. [PubMed: 10228260]
53. Mazariegos GV, Abu-Elmagd K, Jaffe R, et al. Graft versus host disease in intestinal transplantation. Am J Transplant 2004;4:1459–1465. [PubMed: 15307833]
54. Malki A, ElRuz RA, Gupta I, et al. Molecular mechanisms of colon cancer progression and metastasis: recent Insights and Advancements. Int J Mol Sci 2020;22:130. [PubMed: 33374459]
55. Khan FH, Dervan E, Bhattacharyya DD, et al. The role of nitric oxide in cancer: Master regulator or NOt? Int J Mol Sci 2020;21:9393. [PubMed: 33321789]
56. Tang Z, Bauer JA, Morrison B, et al. Nitrosylcobalamin promotes cell death via S nitrosylation of Apo2L/TRAIL receptor DR4. Mol Cell Biol 2006;26:5588–5594. [PubMed: 16847314]
57. Leon-Bollotte L, Subramaniam S, Cauvard O, et al. S-nitrosylation of the death receptor fas promotes fas ligand-mediated apoptosis in cancer cells. Gastroenterology 2011;140:2009–2018, 2018.e1–4. [PubMed: 21354149]
58. Li J, Billiar TR, Talanian RV, et al. Nitric oxide reversibly inhibits seven members of the caspase family via S-nitrosylation. Biochem Biophys Res Commun 1997;240:419–424. [PubMed: 9388494]
59. Nakaizumi A, Horie T, Kida T, et al. Nitric oxide potentiates TNF-α-induced neurotoxicity through suppression of NF-κB. Cell Mol Neurobiol 2012;32:95–106. [PubMed: 21833550]
60. Iorga A, Donovan K, Shojaie L, et al. Interaction of RIPK1 and A20 modulates MAPK signaling in murine acetaminophen toxicity. J Biol Chem 2021;296:100300. [PubMed: 33460648]
61. Priem D, Devos M, Druwé S, et al. A20 protects cells from TNF-induced apoptosis through linear ubiquitin-dependent and -independent mechanisms. Cell Death Dis 2019;10:692. [PubMed: 31534131]
62. Tavares RM, Turer EE, Liu CL, et al. The ubiquitin modifying enzyme A20 restricts B cell survival and prevents autoimmunity. Immunity 2010;33:181–191. [PubMed: 20705491]
63. Kattah MG, Shao L, Rosli YY, et al. A20 and ABIN-1 synergistically preserve intestinal epithelial cell survival. J Exp Med 2018;215:1839–1852. [PubMed: 29930103]

Author Manuscript Author Manuscript Author Manuscript Author Manuscript

64. el Marjou F, Janssen KP, Chang BHJ, et al. Tissue-specific and inducible Cre-mediated recombination in the gut epithelium. Genesis 2004;39:186–193. [PubMed: 15282745]

65. Kim JJ, Shajib MdS, Manocha MM, et al. Investigating intestinal inflammation in DSS-induced model of IBD. J Vis Exp 2012;3678. [PubMed: 22331082]

66. Schindelin J, Arganda-Carreras I, Frise E, et al. Fiji: an open-source platform for biological-image analysis. Nat Methods 2012;9:676–682. [PubMed: 22743772]

67. Sato T, van Es JH, Snippert HJ, et al. Paneth cells constitute the niche for Lgr5 stem cells in intestinal crypts. Nature 2011;469:415–418. [PubMed: 21113151]

68. Sato T, Vries RG, Snippert HJ, et al. Single Lgr5 stem cells build crypt-villus structures in vitro without a mesenchymal niche. Nature 2009;459:262–265. [PubMed: 19329995]

69. Ramirez-Gonzalez RH, Leggett RM, Waite D, et al. StatsDB: platform-agnostic storage and understanding of next generation sequencing run metrics. F1000Res 2013;2:248. [PubMed: 24627795]

70. Bolger AM, Lohse M, Usadel B. Trimmomatic: a flexible trimmer for Illumina sequence data. Bioinformatics 2014;30:2114–2120. [PubMed: 24695404]

71. Dobin A, Davis CA, Schlesinger F, et al. STAR: ultrafast universal RNA-seq aligner. Bioinformatics 2013;29:15–21. [PubMed: 23104886]

Author Manuscript Author Manuscript Author Manuscript Author Manuscript

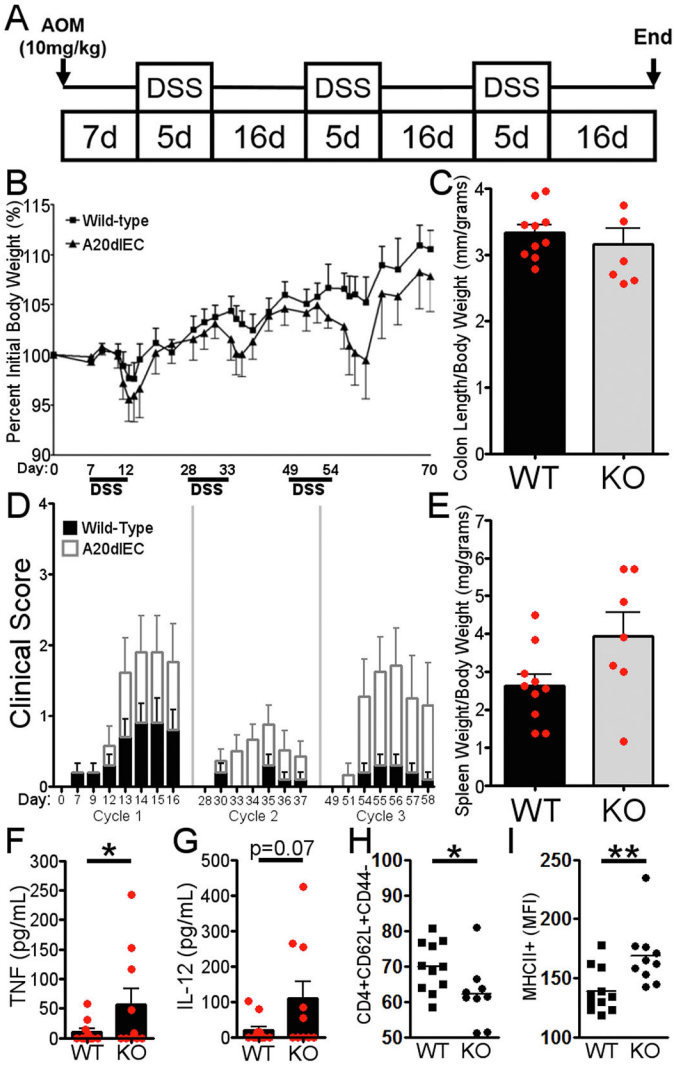

Figure 1.

Phenotype of IEC-specific A20-deficient mice treated with AOM-DSS. (A) Schematic diagram of experimental design. Mice were injected at day 0 with 10 mg/kg AOM. Three rounds of treatment were performed with 1.75% DSS with a sixteen-day interval between each treatment. Mice were euthanized and tissues collected after a total of 70 days. (B) Body weight in wild-type (boxes) and A20dIEC (triangles) expressed as a percentage of initial body weight. Periods of treatment with DSS are shown on the x-axis. Only upper error bars for wild-type and lower error bars for A20dIEC mice are shown for clarity. (C) Colon length normalized to total body weight at the conclusion of the experiment on day 70 in WT and A20dIEC (KO) mice. (D) Average clinical scores for wild-type (black bars) and A20dIEC (open grey bars) during each cycle of DSS. Clinical scores range from 0 to 4 (see methods). (E) Spleen weights normalized to total body weight at the conclusion of the experiment on day 70 in WT and A20dIEC (KO) mice. (F) Serum TNF from WT and A20dIEC (KO) mice at the conclusion of the experiment on day 70 as measured by enzyme-linked immunosorbent assay. (G) Serum interleukin 12 from WT and A20dIEC (KO) mice at the conclusion of the experiment on day 70 as measured by ELISA. (H) Naive

Author Manuscript Author Manuscript Author Manuscript Author Manuscript

splenic T cells ($CD3^+CD4^+CD62L^+CD44^-$) in WT and A20dIEC (KO) mice as determined by flow cytometry. Results are displayed as a percentage of total $CD4^+$ T cells. (I) Mean fluorescence intensity of MHC class II expression on CD11b+Gr-1 low monocytes in the spleen of WT and A20dIEC (KO) mice as determined by flow cytometry. $*P < .05$, $**P < .01$. Comparison between 2 groups was performed by two-tailed unpaired Student's *t*-test. Multigroup comparisons were performed by one-way analysis of variance. n = 3-5 WT and n = 3–5 A20dIEC mice per experiment. Experiments were repeated 3 times. In total, 11 WT males, 4 WT females, 9 A20dIEC males, and 5 A20dIEC females were analyzed.

Author Manuscript Author Manuscript Author Manuscript Author Manuscript

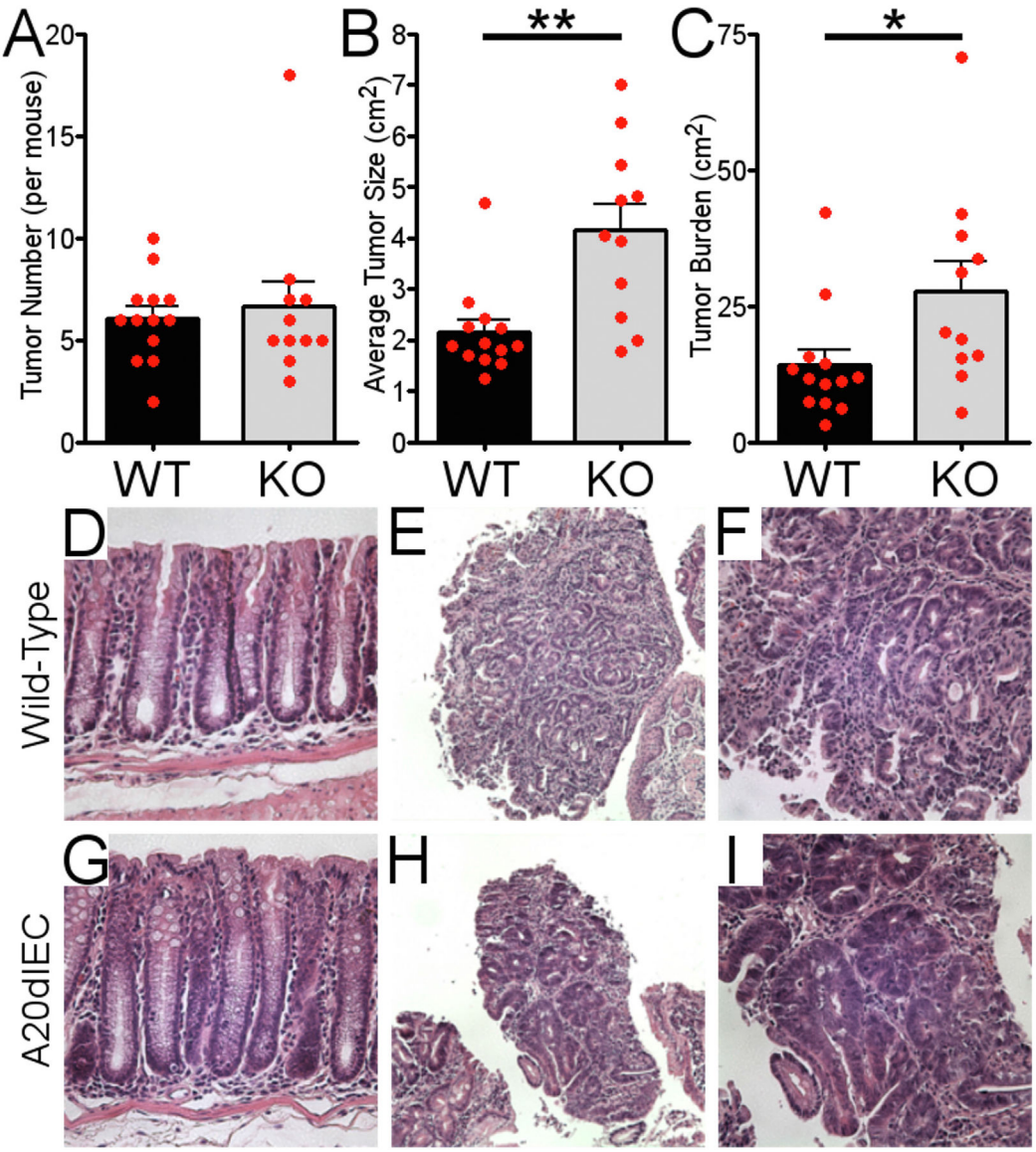

Figure 2.

Increased tumor burden in A20dIEC mice treated with AOM-DSS. (A) Tumor number per mouse in WT and A20dIEC (KO) mice. (B) Average tumor size in WT and A20dIEC (KO) mice. (C) Total tumor burden per mouse in WT and A20dIEC (KO) mice. Tumor burden was calculated by multiplying the tumor number by the average tumor size. (D–I) Representative histologic images from WT (D–F) and A20dIEC (G–I) mice. Normal areas of colon (D, G) and areas of dysplasia (E, H) are shown at 20X magnification. Areas of dysplasia shown at 40X magnification (F, I). *$P < .05$, **$P < .01$. Comparison between 2 groups was performed by two-tailed unpaired Student's *t*-test. Multigroup comparisons were performed by one-way analysis of variance. n = 3–5 WT and n = 3–5 A20dIEC mice per experiment as in Figure 1. Experiments were repeated 3 times.

Author Manuscript Author Manuscript Author Manuscript Author Manuscript

A

Gene Name	Symbol	Fold change
Retinol Dehydrogenase	Rdh9	-6.87
Ubiquitin Specific Peptidase 18	Usp18	-6.58
Inducible Nitric Oxide	Nos2	-6.04
Heat Shock Protein Family B Member 1	Hspb1	-5.21
Plasminogen Activator, Tissue Type	Plat	-4.29
N-acetylglutamate Synthase	Nags	3.25
Synaptotagmin Like 4	Sytl4	3.37
Aldehyde Dehydrogenase 1 Family Member A1	Aldh1a1	4.94
Cytochrome pP450 Family 3 Subfamily A Member 7	Cyp3a13	5.35
Fatty Acid Binding Protein 2	Fabp2	6.78

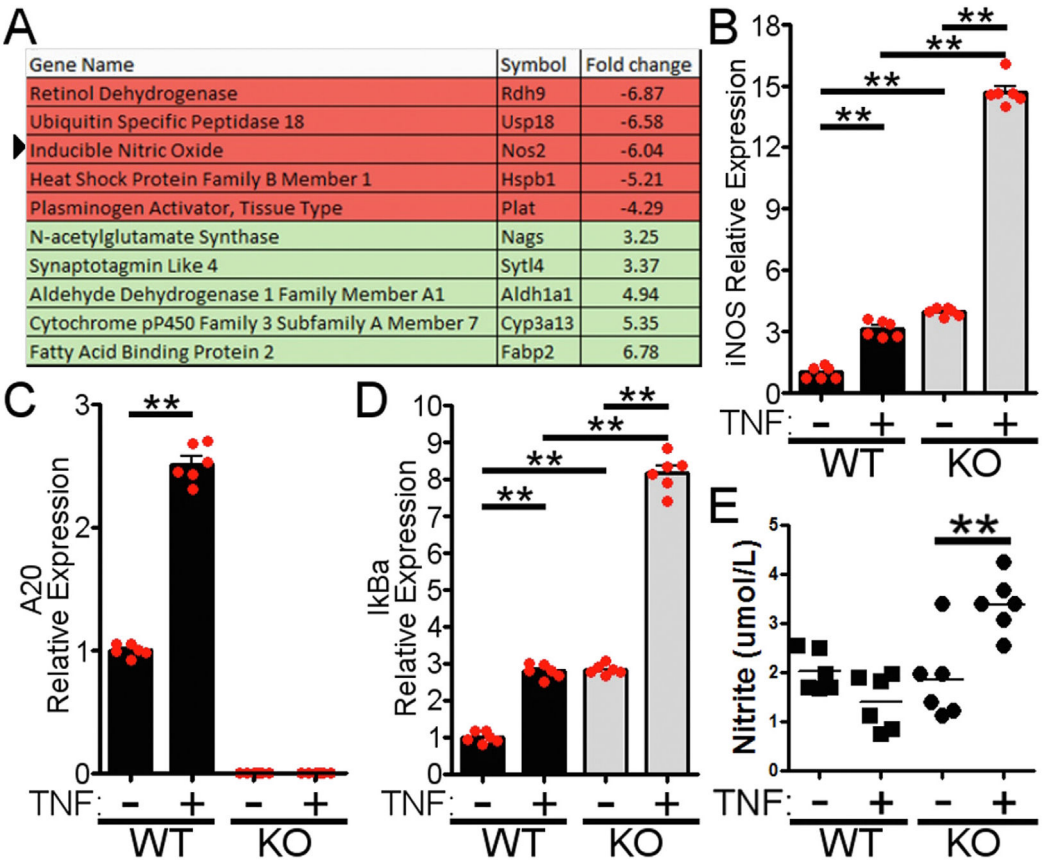

Figure 3.

Upregulation of NOS2 in IEC-specific A20-deficient enteroids after an inflammatory stimulus. (A) The top 5 most highly upregulated (top) and downregulated (bottom) genes in WT vs A20dIEC-derived small intestinal enteroids stimulated with TNF (10 ng/ml) for 24 hours determined by RNAseq. Arrow highlights the expression of inducible nitric oxide (iNOS/NOS2). (B–D) Expression of iNOS (B), A20 (C), and IKBa (D) in WT and A20dIEC (KO)-derived colonic enteroids stimulated with and without TNF (10 ng/ml) for 24 h. (E) Total nitrite level in the supernatants of WT and A20dIEC (KO)-derived colonic enteroids stimulated with and without TNF (10 ng/ml) for 24 hours as determined by Griess reaction. $^{**}P < .01$. Comparison between 2 groups was performed by two-tailed unpaired Student's *t*-test. Multigroup comparisons were performed by one-way analysis of variance. All experiments shown are representative of at least 3 independent experiments.

Author Manuscript Author Manuscript Author Manuscript Author Manuscript

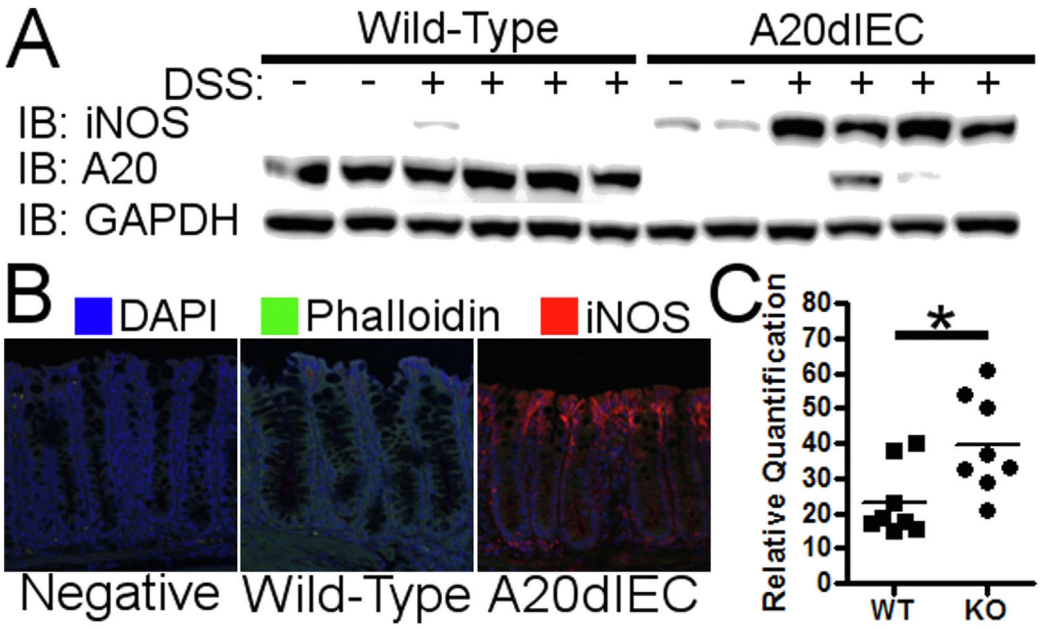

Figure 4.

NOS2 is upregulated in the epithelial cells of IEC-specific A20-deficient mice treated with AOM-DSS. (A) Expression of iNOS, A20, and GAPDH (loading control) by Western blot of intestinal epithelial cells isolated from colonic tissue in WT or A20dIEC mice treated for 3 days with DSS or untreated. (B) Representative immunofluorescence images taken from WT or A20dIEC colons after AOM-DSS treatment. (C) Quantification of iNOS expression in the colonic epithelium of WT or A20dIEC (KO) mice after AOM-DSS treatment. $*P < .05$. Comparisons between 2 groups were performed by two-tailed unpaired Student's *t*-test. Multigroup comparisons were performed by one-way analysis of variance. All experiments shown are representative of at least 3 independent experiments.

Author Manuscript Author Manuscript Author Manuscript Author Manuscript

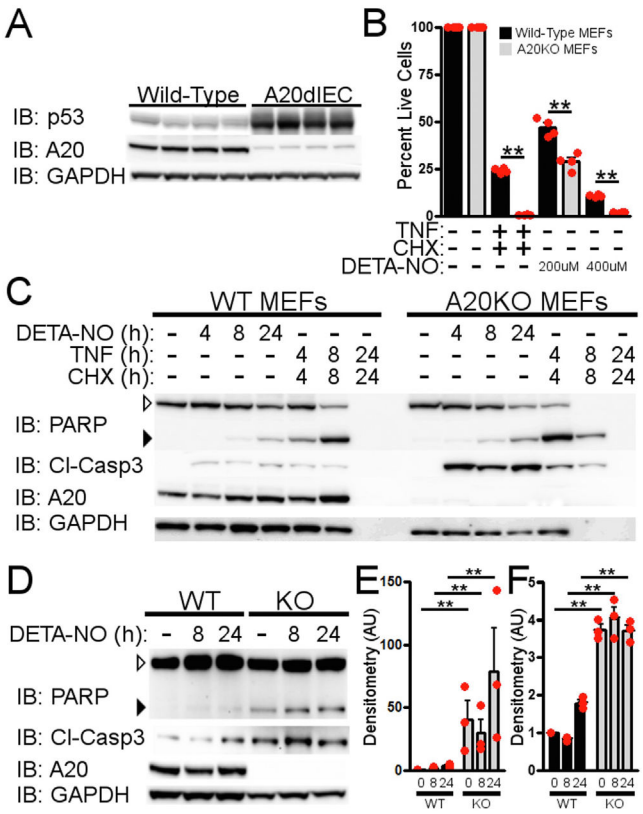

Figure 5.

A20 deficiency enhances susceptibility to DETA-NO cell death. (A) Expression of p53, A20, and GAPDH (loading control) in WT or A20dIEC whole colonic lysates from mice treated with AOM-DSS. (B) Cell death in WT or A20-deficient (A20KO) mouse embryonic fibroblasts (MEFs) treated with TNF (10 ng/ml) and cycloheximide (CHX, 10 μg/ml) or DETA-NO at the indicated concentrations for 24 hours as measured by Cell-Titer Glo assay. (C) Expression of PARP, cleaved-caspase 3 (Cl-Casp3), A20, and GAPDH (loading control) in WT and A20-deficient (A20KO) MEFs stimulated with TNF (10 ng/ml) and CHX (10 μg/ml) or DETA-NO (200 μM) for the indicated times as measured by Western blot. Open arrowhead and closed arrowhead highlight full-length and cleaved PARP, respectively. (D) Expression of PARP, cleaved-caspase 3 (Cl-Casp3), A20, and GAPDH (loading control) in WT and A20-deficient (KO) colonic enteroids stimulated with DETA-NO (200 μM) for the indicated times as measured by Western blot. Open arrowhead and closed arrowhead highlight full-length and cleaved PARP, respectively. (E, F) Densitometry of cleaved PARP (E) and cleaved caspase-3 (F) from Western blot shown in D. $^{**}P < .01$. Comparisons between 2 groups were performed by two-tailed unpaired Student's t-test. Multigroup comparisons were performed by one-way analysis of variance. All experiments shown are representative of at least 3 independent experiments.

Author Manuscript Author Manuscript Author Manuscript Author Manuscript

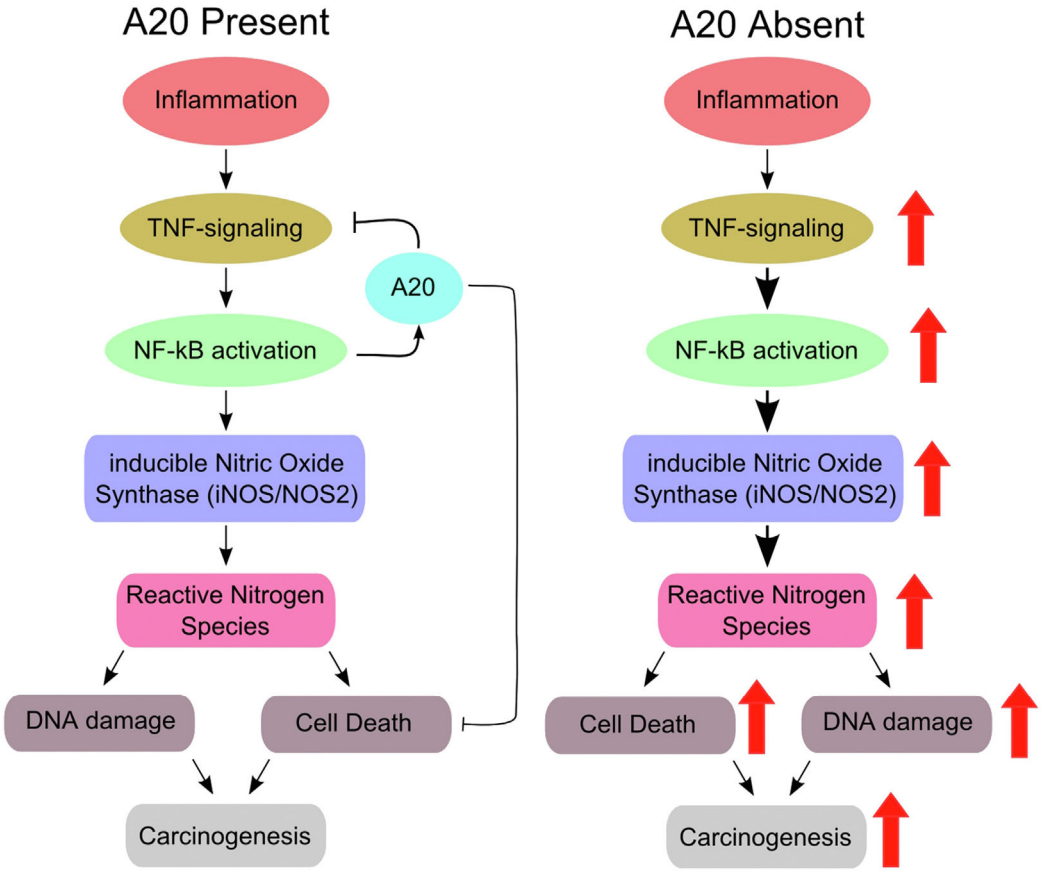

Figure 6.

Proposed model for the regulation of colitis-associated cancer by intestinal epithelial cell expression of A20. Inflammation, for example mediated by TNF, leads to the NFkB-dependent upregulation of inducible nitric oxide synthase (iNOS/NOS2). iNOS can produce reactive nitrogen species which can lead to DNA damage and cell death potentially promoting carcinogenesis. A20 is an early NFkB-induced gene and can dampen further inflammation by restricting TNF-receptor signaling in a classical negative feedback loop leading to decreased expression of iNOS but may also restrict nitric oxide–dependent cell death directly. In the absence of A20, enhanced NFkB activity may lead to increased expression of iNOS and increased production of reactive nitrogen species leading to greater DNA damage. In combination with enhanced nitric oxide–dependent cell death in the absence of A20, carcinogenesis is amplified.

Author Manuscript Author Manuscript Author Manuscript Author Manuscript

Table 1.

Primers Used in This Study

msNOS2	
msNOS2-5 Fwd	TCAGGAAGAAATGCAGGAGATG
msNOS2-5 Rev	TGAACGTAGACCTTGGGTTTG
msA20	
msA20 Fwd	CTGACCTGGTCCTGAGGAAG
msA20 Rev	GAAAAGTCCTGTTTCCACAA
msNFKBIA	
msNfkbia Fwd	TGAAGGACGAGGAGTACGAGC
msNfkbia Rev	TGCAGGAACGAGTCTCCGT
msGAPDH	
msGapdh-2 Fwd	AGGTCGGTGTGAACGGATTTG
msGapdh-2 Rev	TGTAGACCATGTAGTTGAGGTCA